

Assessment of the Performance of Bifacial Solar Panels

Alaa H. Salloom, Omar A. Abdulrazzaq, Ban H. Ismail

Abstract— In this work, a double-sided solar panel (bifacial solar cell configuration) comprising of two silicon PV panels attached back-to-back was investigated. The module was fixed on an adjustable ground mounted frame and the tilt angle was varied to be (30°, 45°, 60°, and 90°). For each angle, temperature and irradiance were monitored in a sunny day at noon in the mid of July in Baghdad city. The photovoltaic performance of each individual panel shows a remarkable variation with tilt angle which attributed to the impact of irradiance and surface temperature of each panel. This impact was anticipated based on Shockley & Queisser principle and Burech equation. The results revealed that the rear panel is performing better than the front panel. Despite that the rear panel was exposed to a lower illumination, it supplied higher power conversion efficiency than this of the front panel except for the case of 90° tilt angle. Bifacial characteristics were studied on the bases of series and parallel connections. The series connection produced lower gain in power than that of the parallel connection.

Index Terms— Bifacial, Silicon solar panel, tilt angle.

I. INTRODUCTION

Solar cell research and development had introduced wide varieties of architectures such as heterojunction solar cells [1], and organic solar cells [2]. However, single crystal silicon solar cell technology is the most proven one and occupies about 90% of the total PV shipment. Despite there were 64 years have elapsed, since the demonstration of the first silicon solar cell [3], the intensive investigations on this device are still current up-to-date. The thermodynamic limit of p-n junction silicon solar cell (so-called Shockley limit) restrains the output power per unit area. The monojunction silicon cell is fundamentally restricted to a ~33% maximum efficiency [4]. This limitation is ruled by the unabsorbed photons with energy less than the silicon bandgap and/or the phonon loss due to the absorption of photons with energy higher than the silicon bandgap. Under some circumstances, the PV station is limited by a finite area. Therefore, the alternative configuration of silicon solar cell is required to increase the output power per unit area. One of the suggestions is to invest the background light scattered from the ground (albedo) and hit the backside of the panel. In the conventional silicon solar cells, the top surface is the only side that sunlight is being absorbed and converted into electricity. Backside is typically coated with an opaque layer of metal contact that cannot absorb any light. In order to capture the albedo, a metallic grid

is deposited onto the backside of the cell instead of a blanket of metal layer. The backside is either over doped (p^{++}) to create a back-surface-field or it is doped with a donor impurity to create a p-n junction on the back. This configuration allows the background light to penetrate the backside of the cell and then being converted into electricity. The additional light absorbed through the backside of the cell leads to enhanced electrical power generation. This architecture is referred to as a bifacial solar cell.

Bifacial solar cell was first patented by the end of 1979 [5]. Even though, few literature is available on this architecture of solar cells [6], [7], [8], [9]. This type of cell is an active for both sides. In silicon solar cell, the semiconductor substrate could be n-type or p-type. Here we have a polycrystalline of two individual solar panels; attached back-to-back to invest the albedo irradiance and then to enhance the output power per unit area.

Solar cells on the house roof suffer from the wide variety of operating temperatures (often in the range between 0-70°C). Thus, it is urgent and imperative to study the effect of ambient temperature on the bifacial solar panel characteristics. This effect is rarely taken into account when the cell parameters are determined in the research labs.

The aim of this research is to present the development and comparison of bifacial solar cells produced by stacking two monofacial solar panels in reverse direction. The front face receives a direct solar irradiance and the rear face receives an indirect solar irradiance that reflected from clouds, ground, and from the buildings around. The main thrust is devoted to study the effect of ambient temperature on bifacial PV panels' performance. The important photovoltaic parameters (viz; short circuit photocurrent density J_{SC} , open circuit photovoltage V_{OC} , fill factor FF, maximum power conversion efficiency PCE, series resistance R_S , and shunt resistance R_{Sh} under illumination) were investigated for the bifacial system in a hot summer day in Baghdad city.

II. EXPERIMENTAL PROCEDURE

The data were collected in Baghdad city (33.3128°N, 44.3615°E coordinates) at noon in the mid of July. In this date, time, and location, the sun is at 119° azimuth angle and 71° altitude angle [10].

Two solar modules of polycrystalline silicon p-n junction made on a p-type wafer were used in this study. The two panels were attached back-to-back and fixed on an adjustable ground mounted frame at a height of 0.5m. The system was fixed directly to the south so that the front side will be facing south while the rear side will be oriented to the ground as shown in Figure (1). Four tilt angles (30°, 45°, 60°, and 90°) were investigated in this work. These angles were adjusted manually according to the pre-designed frame with suitable rivets.

Alaa H. Salloom, Renewable Energy and Environment Research Center/ Corporation of Research and Industrial Development/ Ministry of Industry and Minerals, Baghdad, Iraq

Omar A. Abdulrazzaq, Renewable Energy and Environment Research Center/ Corporation of Research and Industrial Development/ Ministry of Industry and Minerals, Baghdad, Iraq

Ban H. Ismail, Renewable Energy and Environment Research Center/ Corporation of Research and Industrial Development/ Ministry of Industry and Minerals, Baghdad, Iraq

The panels were measured outdoor using Prova-200 PV portable module analyzer. This analyzer provides the user with the swept current and voltage data as well as the other parameters such as maximum solar power, current and voltage at maximum power, open circuit voltage and short circuit current. Solar cell efficiency and fill factor were also calculated from the measured data. The panel's surface temperature and the sunlight illumination during the experiment were determined using a solar power meter type (SPM-1116S) and an environmental meter type (Extech EN300) respectively.



Figure (1). The double sided solar panel used in this study. The rear panel (right) was facing the ground when the front panel (left) is facing south.

Data were collected at different times in the same day and for different days as well in various tilt angles to get accurate comparison for the effect of tilt angle, temperature and the intensity of the incident and reflected sunlight on the performance of the double-sided solar panel.

The type of the ground has a significant effect on the intensity of reflected radiation on the rear panel which in turns affects the amount of energy obtained from the rear panel. In this study, we fixed the system on a concrete floor with no paint on it.

III. RESULTS AND DISCUSSION

The solar irradiance (solar power density) at various tilt angles measured by a standard silicon power meter is illustrated in Figure (2). The direct exposure represents the incident solar power density fallen directly onto the surface at a given angle, while the diffused exposure represents the solar power density reflected from the ground back into the rear side of the surface. Since the rear surface is shadowed, the solar irradiance will be less than that of the direct exposure. The figure shows that irradiance in the shadow is about five folds less than that of direct exposure at 30° tilt angle. Although, the disparity is reduced with increasing tilt angle and the irradiance on both sides becomes close at 90° tilt angle. At 30° tilt angle, the irradiance reaches to 825W/m², a near value to the AM1.5G standard irradiance (1000W/m²). This is because the sun's altitude at the measurements date and time is 71°. At 30° tilt angle, the solar incident beam angle on the panel's surface will be 11° which is nearly perpendicular to the surface of the panel.

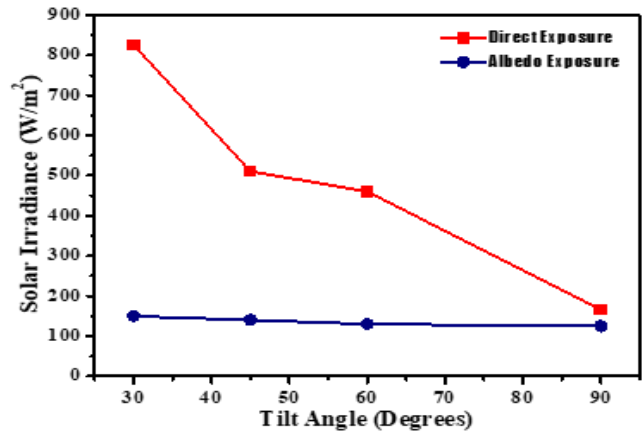


Figure (2). Solar Irradiance vs tilt angle for both direct and albedo exposure.

Figure (3) demonstrates the variation of surface temperature at various tilt angles monitored by using the k-type thermocouple. The front surface incurs higher temperature compared to rear surface. The front surface temperature at 30° tilt angle, for instance is 57°C, while it is 48.5°C for the rear surface at the same tilt angle which is 8°C temperature difference. This difference is considered significant in solar cell operation and can affect dramatically on the cell performance. When the tilting angle increases, the surface temperature decreases slightly. However, the irradiance hitting the panel decreases with increasing the tilt angle as well as presented earlier in Figure (2). This can suggest that the benefit of decreasing surface temperature will be hampered by the reduction in the solar irradiance.

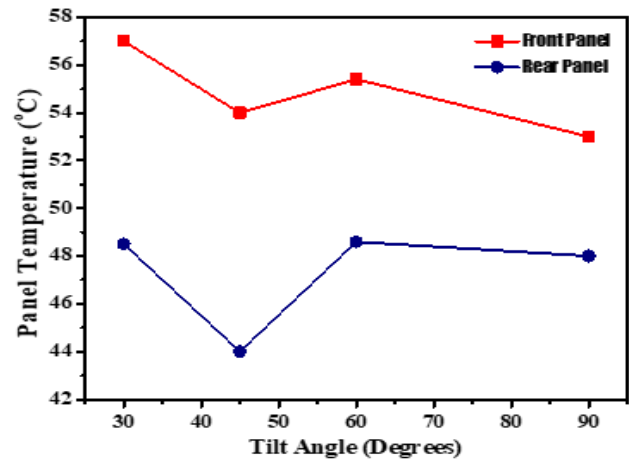


Figure (3). Surface temperature vs tilt angle for direct and albedo exposure.

The fourth quadrant JV curves of the front and rear solar panels at various tilt angles are illustrated in Figure (4). It is clearly visible that the rear panel is exhibiting better squareness than that of the front panel in this experiment. This can predict that the fill factor and hence, the power conversion efficiency of the rear panel is higher than that of the front panel. The front panel JV curves show a significant deterioration, mainly due to the impact of the high temperature on the front panel (see Figure 3). Even so, the short circuit current of the front panel is way higher than that of the rear panel. This is due to the higher irradiance on the front panel (see Figure 2). On the other hand, the open circuit voltage of the front and rear panels shows a slight difference which will be discussed elsewhere.

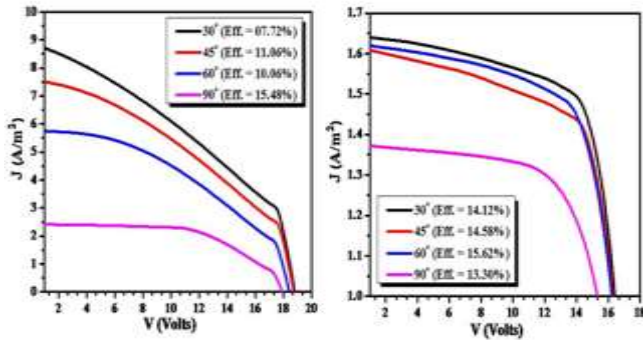


Figure (4). JV curves for front (left) and rear (right) solar panels at various tilt angles.

The photovoltaic performance of the front and rear panels at various tilt angles is demonstrated in Figure (5 a, b, c, & d). Since the front panel is illuminated with a higher irradiance than the rear panel (about five folds higher), it provides higher V_{OC} and J_{SC} as shown in Figure (5 a & b). However, the PCE and FF of the rear panel are interestingly higher than their corresponding values of the front panel. This interesting result can be ascribed directly to the panel's temperature. The higher temperature of the front panel (~8°C higher than the rear) reduces the overall performance of the front panel leading to a lower PCE and a lower FF as shown in Figure (5 c & d). This result suggests that silicon solar panels can introduce higher efficiency in the shade than under the sun in the extremely hot weather. The exception is the 90° tilt angle where the PCE of the front panel exceeds that of the rear panel. This is because both panels have close values of temperature at this specific angle. To investigate the effect of temperature on the power conversion efficiency of a solar cell, the so-called "detailed balance principle" established by Shockley & Queisser can be used [4]. Based on this principle, the recombination process of the solar cell is increased by increasing temperature. The assumption is that every recombination creates a photon and this process can be thought up as a photon recycling. Therefore, the net of the photo-generated carriers extracted out of the cell will be reduced. Consequently, the power conversion efficiency of the device will be reduced.

As tilt angle increases, both V_{OC} and J_{SC} decrease for both front and rear panel. As presented earlier in Figures (2 & 3), both irradiance and temperature decrease with increasing tilt angle, which means: at small tilt angles (namely 30°), irradiance and temperature are at their highest. Burech's equation [11] developed from Shockley model of the diode can be used to investigate the impact of irradiance and temperature on V_{OC} and J_{SC} :

$$I_{SC} = [I_{SCr} + K_I(T_{Panel} - T_r)] \frac{G}{G_r} \quad (1)$$

$$V_{OC} = V_{OCr} + K_V(T_{Panel} - T_r) \quad (2)$$

where: T_r is the standard ambient temperature (25°C), T_{Panel} is the actual panel's temperature, I_{SCr} & V_{OCr} are short circuit current and open circuit voltage, respectively at the standard conditions (1000W/m², temp. 25°C), K_I & K_V are the I_{SC} & V_{OC} temperature coefficients respectively, G_r is the standard irradiance (1000W/m²), and G is the actual irradiance. Equation (1) shows that I_{SC} is a temperature and irradiance dependent parameter where it obeys a direct relationship with

T and G . This equation agrees well with the behavior of Figure (5 a). V_{OC} however, shows a slight increase with tilt angle as illustrated in Figure (5 b). V_{OC} shows no dependence on irradiance and it is linearly proportional to temperature only as expressed in Equation (2). V_{OC} is arising from the built-in potential at the junction which in turns is a function of doping concentration and the junction properties in which irradiance has no influence on these parameters. Basically, increasing temperature reduces the band gap of the silicon according to Varshni's empirical equation [11] (Equation 3) which results in an increase in the saturation current (so-called leakage current) according to Shockley's model (Equation 4) [12]:

$$E_g(T) = E_g(0) - \frac{\alpha T^2}{T + \beta} \quad (3)$$

$$I_s = AT^3 \exp\left(-\frac{E_g}{nkT}\right) \quad (4)$$

where: $E_g(0)$ is the silicon band gap at zero Kelvin, α & β are fitting parameters characterized by the material, I_s is the saturation current (leakage current), A is Shockley constant of silicon, E_g is the silicon band gap at the given temperature, n is the ideality factor of the diode, k is Boltzmann constant, and T is temperature in Kelvin. The V_{OC} is correlated logarithmically with I_s by the following equation [12]:

$$V_{OC} = \frac{kT}{q} \ln \left[\frac{I_{SC}}{I_s} \right] \quad (5)$$

As the temperature and irradiance rise up, both I_{SC} and I_s will increase with a domination in I_s (Equation 4). I_s doubles in magnitude for each 10°C rise in temperature. As a result, the logarithmic part of Equation (5) will decrease. That decrease will be compensated by an increase in T in the same equation and the resultant demonstrates a slight increment in V_{OC} .

Temperature affects series resistance (R_s) and shunt resistance (R_{sh}). These parameters can be extracted from the JV curve by taking the reciprocal of slopes of the J_{SC} region and V_{OC} region to estimate R_{sh} and R_s respectively, as depicted in Figure (6). In the ideal solar cell, $R_s = 0$ and $R_{sh} = \infty$. Substantial amount of R_s and finite amount of R_{sh} in actual cell will reduce the fill factor to less than unity (the ideal Shockley diode). The reduction in FF causes a reduction in power conversion efficiency. Both R_s and R_{sh} of the front and rear panels were calculated by using OriginLab software to obtain precise results.

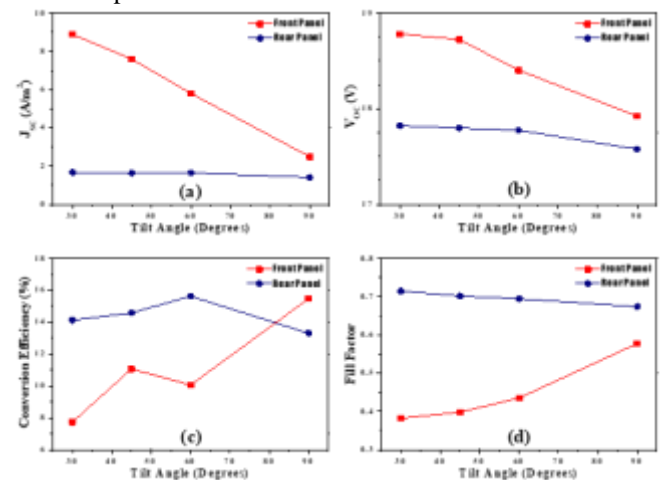


Figure (5). Photovoltaic parameters of the front and rear panels namely: J_{SC} (a), V_{OC} (b), PCE (c), and FF (d).

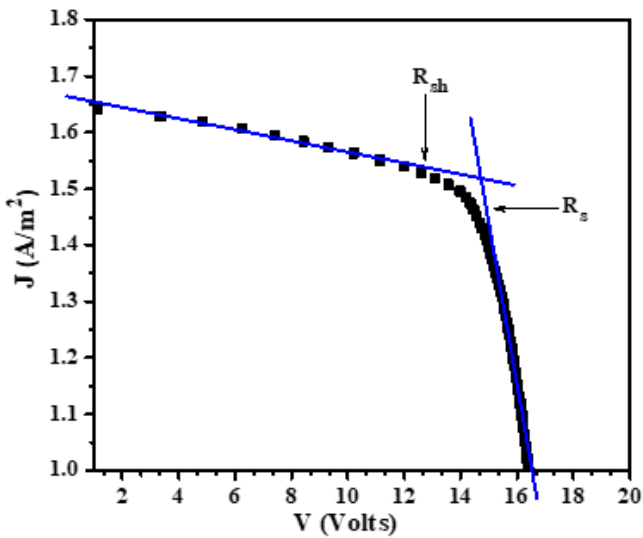


Figure (6). The method used to calculate series and shunt resistances.

The series and shunt resistances of the front and rear panels as a function of solar irradiance are illustrated in Figure (7). As shown in the figure, series resistance for both panels increases with tilt angle. Since the current increases with irradiance (Equation 1), and smaller tilt angles introduce higher irradiance (Figure 2), the current will be higher at smaller tilt angles and consequently, the series resistance will be smaller. However, series of the front panel exhibits sharper decrease with decreasing tilt angle. This can be attributed to the higher temperature and irradiance at smaller tilt angles that boosts more current (Equation 1).

Shunt resistance for both panels shows a decrease with decreasing tilt angle but tends to taper off after the 60° tilt angle. At 30° tilt angle, shunt of the rear panel rises up a tad. This result reveals that irradiance and temperature have no clear effect on shunt resistance for both panels.

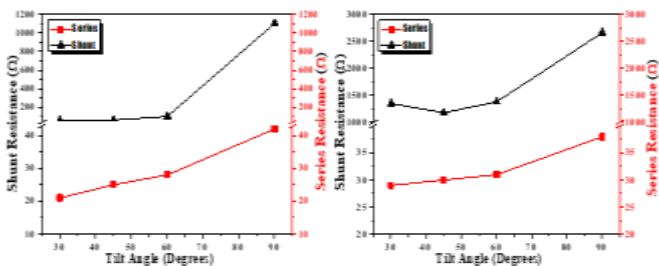


Figure (7). Series and shunt resistances of the front panel (left) and rear panel (right) as a function of tilt angle.

To imitate the bifacial architecture, the output powers of the front and rear panel are combined in series and parallel bases as represented in Figure (8). In series, the current is limited by the lowest current of the two panels, while the voltage is the sum of the two panels' voltages. In parallel, the voltage is limited by the lowest voltage of the two panels, while the current is the sum of the two panels' currents. The power gain resulted from the series or parallel connection is calculated by considering the front panel as the reference panel because the front panel is the panel of the regular direction. Therefore, the gain will be in the form [13]:

$$\text{Gain} = \frac{P_{\text{Series/Parallel}} - P_{\text{Front}}}{P_{\text{Front}}} \times 100\% \quad (6)$$

The series connection exhibits poor output power compared to the parallel connection. Since the voltage introduces smaller diversity with tilt angle compared to the current (Figure 5 a & b), series connection will be affected negatively because it is ruled by the steep variation of the current. The parallel connection on the other hand, is ruled by the gentle variation of the voltage, so it gives higher output power and gain. It is worth mentioning that the gain in series connection has negative values at all angles less than 90° indicating that parallel connection should be applied in the bifacial architecture in the extremely hot weather. The bifacial system in parallel connection enhances the power collection and hence provides higher power per unit area. This can help reducing the panels' area at the site.

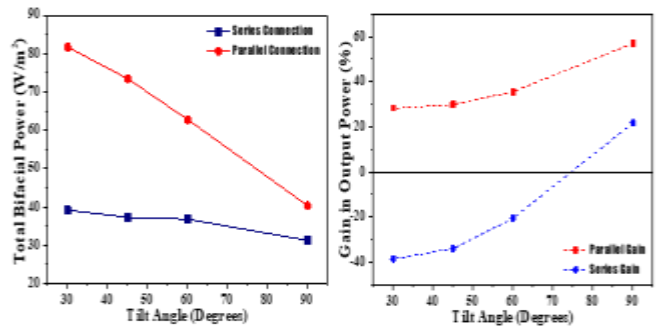


Figure (8). Total bifacial power (left) and output power gain (right) of the two panels connected on series or on parallel.

The quality of the bifacial system is called "bifaciality" and is defined as the ratio of the maximum rated power when the bifacial system is irradiated from the rear to that from the front [14]:

$$\text{Bifaciality} = \frac{P_{m(\text{Rear})}}{P_{m(\text{Front})}} \quad (7)$$

The ideal system presents a bifaciality of unity. In the reality, the system gives a good bifacial quality if the bifaciality is as close as to unity. Figure (9) shows that the best bifacial quality is at 90° in which the temperature difference between the two panels is the smallest. Generally speaking, bifaciality is improved with increasing the tilt angle. The total output power is at its highest at small tilt angle (namely 30°) because the front panel is receiving higher irradiance at small angles whereas rear panel is receiving smaller irradiance, but the energy harvested will be at its highest at 90°.

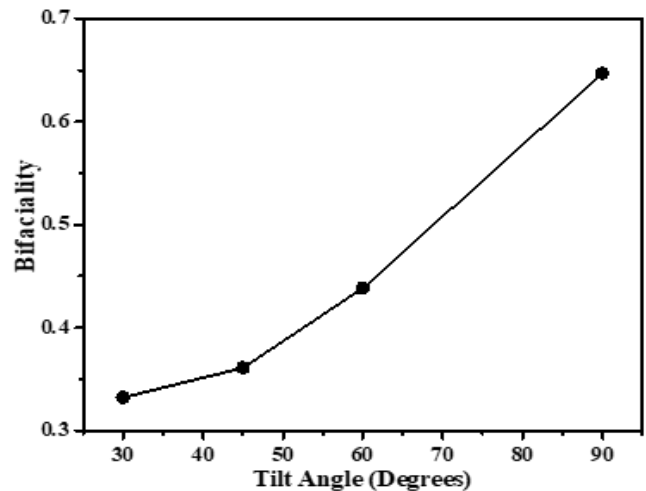


Figure (9). Bifaciality of the bifacial system as a function of tilt angle.

IV. CONCLUSIONS

From what has been discussed, it can be concluded that photovoltaic performance of bifacial silicon solar panel is very sensitive to the operating temperature. The panel exposed to the albedo can provide higher efficiency than that of direct exposure in the hot weather because the surface temperature can be dropped to up to $\sim 8^{\circ}\text{C}$ compared to the front surface temperature. The results also showed that parallel connection can provide higher power than the series connection of the system. The power gain in series connection is less than zero except for 90°C tilt angle, while in parallel connection the gain exceeds 25% for all tilt angles used in this study. The influence of various types of grounds (such as grass, whitened floor, and unpaved floor) on the photovoltaic performance of the bifacial solar cell is under progress.

REFERENCES

- [1] R. A. Ismail, K. I. Hassan, O. A. Abdulrazaq, and W. H. Abode, "Optoelectronic properties of CdTe/Si heterojunction prepared by pulsed Nd:YAG-laser deposition technique," *Mater. Sci. Semicond. Process.*, vol. 10, no. 1, pp. 19–23, 2007.
- [2] R. Punnamchandrar et al., "Triplet Sensitizer Modification of Poly(3-hexyl)thiophene (P3HT) for Increased Efficiency in Bulk Heterojunction Photovoltaic Devices," *Energy Technol.*, vol. 2, no. 7, pp. 604–611, Jun. 2014.
- [3] D. M. Chapin, C. S. Fuller, and G. L. Pearson, "A New Silicon p- n Junction Photocell for Converting Solar Radiation into Electrical Power," *J. Appl. Phys.*, vol. 25, no. 5, pp. 676–677, May 1954.
- [4] W. Shockley and H. J. Queisser, "Detailed Balance Limit of Efficiency of p- n Junction Solar Cells," *J. Appl. Phys.*, vol. 32, no. 3, pp. 510–519, Mar. 1961.
- [5] A. Luque, "Double-Sided Solar Cell With Self-Refrgerating Concentrator," US4169738A, 1979.
- [6] A. Cuevas, A. Luque, J. Eguren, and J. del Alamo, "50 Per cent more output power from an albedo-collecting flat panel using bifacial solar cells," *Sol. Energy*, vol. 29, no. 5, pp. 419–420, 1982.
- [7] V. Poulek and M. Libra, "A very simple solar tracker for space and terrestrial applications," *Sol. Energy Mater. Sol. Cells*, vol. 60, no. 2, pp. 99–103, 2000.
- [8] O. H., S. M., T. K., and Y. Y., "Bifacial silicon solar cells with 21.3% front efficiency and 19.8% rear efficiency," *Prog. Photovoltaics Res. Appl.*, vol. 8, no. 4, pp. 385–390, Aug. 2000.
- [9] W. Zhao et al., "0.35% absolute efficiency gain of bifacial N-type Si solar cells by industrial Metal Wrap Through Technology," in 2012 38th IEEE Photovoltaic Specialists Conference, 2012, pp. 2289–2291.
- [10] Susdesign, "Sun Position," 1998. [Online]. Available: <http://susdesign.com/sunposition/>. [Accessed: 15-Apr-2018].
- [11] M. Arnaout, W. Salameh, and A. Assi, "IMPACT OF SOLAR RADIATION AND TEMPERATURE LEVELS ON THE VARIATION OF THE SERIES AND SHUNT RESISTORS IN PHOTOVOLTAIC MODULES," pp. 295–301, 2016.
- [12] S. M. Sze and K. K. Ng, *Physics of Semiconductor Devices*, Third. John Wiley & Sons, Inc., 2006.
- [13] X. Sun, M. R. Khan, C. Deline, and M. A. Alam, "Optimization and performance of bifacial solar modules: A global perspective," *Appl. Energy*, vol. 212, pp. 1601–1610, 2018.
- [14] P. Ooshaksaraei, K. Sopian, R. Zulkifli, M. A. Alghoul, and S. H. Zaidi, "Characterization of a bifacial photovoltaic panel integrated with external diffuse and semimirror type reflectors," *International Journal of Photoenergy*, vol. 2013, 2013.